Investigating the Impact of Surfactants on Protein Folding: Insights from AF4, DLS and ProbeDrum

Emelie Johansson
2024-05-31

Master Thesis in Pharmaceutical Technology
Department of Process and Life Science Engineering
Faculty of Engineering, Lund University

Supervisor: Lars Nilsson
Examiner: Marie Wahlgren

Abstract

Today, proteins are used in a huge variety of industrial application ranging from detergents and pharmaceuticals to cosmetical products. Surfactants have the potential to increase solubility of poorly soluble protein, as well as hindering proteins in formulation to interact with the interface and thus protecting them from degradation. Even if the use of protein-surfactant system dates back decades and so does the research about them, there is no full understanding of the mechanism behind these system. In order to optimize its applications, a greater understanding of the protein-surfactant interactions need to be established.

Surfactants naturally forms micelles in water, concealing their hydrophobic tails while exposing their hydrophilic heads. Depending on the charge of the surfactant, they are classified as ionic or non-ionic surfactants. Ionic surfactants tend to form micelles at a higher concentration compared to non-ionic surfactants. When combining ionic and non-ionic surfactants, they create mixed micelles. This phenomenon can be utilized by the addition of a non-ionic surfactant to a solution of a protein and an ionic surfactant. Studies have shown that this reverses protein denaturation, restoring the protein to its native and active state. The formation of mixed micelles prevents the ionic surfactant from binding to and denaturating the protein.

However, while the reversal of protein denaturation by non-ionic surfactants have been proved with simpler proteins, its effectiveness with antibodies remains. In this report, addition of both ionic and non-ionic surfactant to an antibody solution was performed. Analysis of the solution with asymmetrical flow field-flow fractionation, dynamic light scattering, fluorescence spectroscopy and static light scattering confirms that this approach is also effective for the antibody, expanding its potential applications and lays the foundation for further optimization.

Acknowledgements

I would like to express my gratitude to my supervisor and examiner for their support and insights during the completion of my master's thesis. Which also concludes my studies in Biotechnology Engineering at Lund University.

My sincere thanks to Lars Nilsson for his mentorship, insightful feedback and support during this challenging yet rewarding project. His guidance has enhanced my understanding of the subject matter. I would also like to thank Hans Bolinsson for all the technical assistance with the AF4 instrument.

I am also grateful of Marie Wahlgren, who not only found this project but also contributed to a successful completion of my master's degree. Her assistance and expertise have been guiding me through the challenges of this project.

Thank you,
Emelie Johansson

Table of contents

1 Introduction

1.1 Overview

Protein-surfactant systems are a crucial part of modern chemistry and are commonly used in the pharmaceutical field. When using a poorly soluble protein the surfactants have the ability to increase solubility of the active ingredient which increases its bio-availability (Das, et al. 2022). Enhanced bio-availability enables the active ingredient to achieve its desired therapeutic effect more efficiently, often leading reduced dosage requirements. For soluble proteins, surfactants are instead mainly used to prevent adsorption to the interface. This protects the protein from degradation and preserve its functionality (Fatma, et al. 2021). Despite that these systems have been studied for decades, the full mechanism behind their interaction have not been established (Fatma, et al. 2021). By understanding the mechanism behind the protein-surfactant interactions, further optimization of current applications could be done and potentially new areas of use could be found.

Surfactants are surface-active molecules that are amphlicic due to their hydrophilic head and hydrophobic tail. In water, surfactants are dependent on their critical micelle concentration, CMC as they form micelles above that concentration (Fatma, et al. 2021). This phenomenon occurs naturally as a result of the hydrophilic head of the surfactant that tends to remain in water, while the hydrophobic tail seeks to minimize contact with water. Which causes the micelles to form spontaneously, with the tails in the core and heads oriented outwards to form a shield. Generally, below the surfactants CMC the protein will be stabilised since the surfactant hinder protein absorption to the interface as well as impending its coagulation. Above the CMC the protein will instead be destabilised and fully or partly denaturated (Fatma, et al. 2021).

Dependent on the charge of the surfactant it will be classified as ionic or non-ionic. This determines the mechanism behind how the surfactant could interact with the protein, which makes the protein-surfactant interactions more complex (Sanchez-Fernandez, et al. 2020). Generally, surfactants only interact with proteins above their CMC, however it has been found that anionic surfactants such as Sodium Dodecyl Sulfate, SDS interacts with proteins well below their CMC, causing the protein to denaturate (Otzen, et al. 2022).

There have been several models trying to explain the protein-surfactant interactions over the years, but the Core-Shell model is the leading one today. The model suggest that micelles are surrounded by partly denaturated proteins. There could be several partly denaturated proteins surrounding one micelle or several micelles could be surrounded by only one larger protein. Exactly how the micelle-protein surrounding look depends on the concentration ratio between surfactant and protein. However, these systems are more complex as they also depend on the pH, temperature and the ionic strength of the protein (Otzen, et al. 2022).

Anionic surfactants can interact with proteins well below their CMC because they are able to build up small clusters with the protein. The anionic head group of the surfactant can associate with the proteins which mitigates the electrostatic repulsion among the surfactant molecules. This causes the surfactant to form clusters like smaller micelles in the presence of protein well below their CMC (Otzen, et al. 2022). However, the association with the protein will cause it to denaturate as it will extend in order to maximize the interaction area with the surfactant (Otzen, et al. 2022). The higher ionic strength of the solution, the more the protein will expand during the unfolding caused by SDS (Otzen 2002). As the concentration of surfactant rise the few surfactants on the protein will form clusters and finally micelles will be formed. At low surfactant concentrations, several proteins can surround one micelle with only a part of the protein interacting with the micelle. However, as concentration of the surfactant rises more micelles will form and finally only one micelle will interact with only one protein.

While both non-ionic and ionic surfactants could interact with water and water-soluble proteins through hydrogen bonding, their main interaction mechanism differ from each other. Non-ionic surfactants generally rely on hydrophobic and hydrogen bond interactions with proteins, while ionic surfactants interact through electrostatic forces which are stronger (Sanches-Fernandes, et al. 2020). This causes non-ionic surfactants to typically not interact with water-soluble proteins as ionic surfactants do. Furthermore, because non-ionic surfactants lack the electrostatic repulsion, they form micelles at a much lower concentration compared to ionic surfactants. Which causes non-ionic surfactants to form micelles rather than interact with the protein.

The denaturation caused by ionic surfactants affects both the proteins secondary and tertiary structure (Poghosyan, et al. 2019). However, it has also been found that this could be reversed. This has been investigated for several less complex proteins, but not for an antibody. By adding sequestering agents, they can take up the surfactant from a solution. However, these agents are hard to control, especially when using low concentrations of surfactant. Instead, a non-ionic surfactant such as Dodecyl-beta-D-maltoside, DDM have been shown to be useful since mixed micelles will form. If added together with an ionic surfactant, the denaturation of the protein will become slower and if added after an ionic surfactant, the denaturation will be reversed and the protein could return to its native state (Otzen, et al. 2022). However, the mechanism seems to be complex since the ionic surfactant sometimes are stripped of directly and other times it requires longer time for the protein to return to its native state (Otzen, et al. 2022). The removal of SDS and refolding of protein occurs in several steps which first removes SDS from the unfolded protein, absorption of SDS to mixed micelles and then steps of refolding the protein into its native state (Pedersen, et al. 2020). The mixed micelles which are formed will contain both ionic and non-ionic surfactants. Since non-ionic surfactant forms micelles at lower concentrations the ionic-surfactants will be taken up by those micelles and therefore not be able to associate with the protein to the same extent. This is advantageous for the ionic surfactant as it will lower its CMC (Otzen 2011). Which is why the denaturation will be more reversed with higher concentrations of non-ionic surfactant present in relation to the ionic surfactant (Kaspersen, et al. 2017).

1.2 Aim & objective

This thesis investigates the protein-surfactant interactions, focusing on the conformational changes the antibody undergoes due to addition of different surfactants. The aim of this thesis is to investigate

- If the ionic surfactant SDS denatures the antibody trastuzumab
- If the denaturation caused by SDS is reversible
- If addition of DDM will reverse the changes SDS causes
- To which extent DDM can reverse the changes SDS causes

2 Background

A prior study at the institution revealed that addition of DDM to a protein solution with SDS will partly reverse the conformational changes of the protein so it could go back to its native state. However, antibodies are commonly used in pharma and it is therefore important to discover if the same conclusion could be drawn for antibodies which are a more complicated protein.

2.1 AF4

Asymmetrical Flow Field-Flow Fractionation, AF4 is similar to chromatography, but does not have a stationary phase. In AF4, a lateral force is applied to a flat channel which forces the liquid through it. By adding a semipermeable membrane into the channel, a cross flow is induced which results in a separation. The separation results in a concentration profile which is determined by the diffusion coefficient of each component. The peak width of the concentration profile represents the distribution of particle sizes or molecular weights within the sample. A narrow peak signifies a concentrated size distribution, while a wider peak suggests a broader range of molecular sizes present. While the area under the peak determines its concentration. Generally, small particles will flow further in the channel than larger particles, allowing the technique to separates solution components based on their size (Maskos, et al. 2011).

2.2 DLS

Dynamic Light Scattering, DLS is a non-invasive technique used to measure size and size distribution of molecules in a sample. It is based on the theory of Brownian motion and uses a laser on the molecules in the sample. As the laser hits the particles, the intensity of scattered light varies depending on the size of the particle. This enables DLS to accurately measure individual particle sizes and size distribution within a sample (Malvern Panalytical 2024).

2.3 Probe Drum

Probe Drum is a multi-detection system which measures fluorescence, absorbance and light scattering of a sample at the same time. During the experiment it is possible to titrate a solution into the sample and detect the changes. Which enables Probe Drum to detect changes the sample undergoes in real time (Labbot 2023).

2.4 Surfactants

Sodium Dodecyl Sulfate, SDS is an ionic surfactant which is commonly used as a surfactant in cosmetic products such as shampoo and creams. However, SDS also has microbicidal activity against virus, but is not approved for this application. The molar weight is 288.37 g/mol (PubChem, SDS) and it has a CMC in water at 25 °C of 8.10 mM (Umlong, et al. 2007).

Dodecyl-beta-D-maltoside, DDM is a non-ionic surfactant commonly used to solubilize and purify proteins of the membrane. The molar weight is 510.62 g/mol

(PubChem, DDM) and it has a CMC in water at 25 °C of 0.17 mM (ThermoFisher Scientific 2024).

2.5 Trastuzumab

Trastuzumab is an antibody used in HER2 cancer treatment since it inhibits growth of the cancer cells (Cancercentrum 2023). Trastuzumab has a molar weight of 145 423 g/mol and a molar extinction coefficient of 209409 M^-1 cm^-1 (Abendi, et al. 2019). The isoelectric point, pI where it carries no net charge is approximately 8.45 for trastuzumab (Xu, et al. 2015).

3 Methodology

The study was carried out at Division of Food and Pharma, Lund University between 2024-02-12 to 2024-04-23.

3.1 Material

For all AF4 experiments a phosphate buffer with a concentration of 10 mM and pH 8 was used as the carrier liquid. The buffer was prepared using sodium phosphate monobasic, sodium phosphate dibasic and MilliQ water. Trastuzumab was consistently used at a concentration of 1 mg/ml in all samples. In samples containing SDS the concentration was either 3.8 mM, 6.25 mM or 12 mM. The concentration of DDM varied based on the SDS concentration, with ratios of 1:1, 1:4, 1:8 and 1:12 relative to the current SDS concentration. The same samples used in AF4 were used in DLS.

In the fluorescence spectroscopy and the static light scattering experiments, the concentration of trastuzumab was at 1 mg/ml for all samples. The first experiment the sample was titrated with 80 mM SDS which gave the sample a final concentration of 20 mM SDS. For the two other experiments, the sample contained SDS at concentration either at 3.8 mM or 6.25 mM and a DDM solution of 144 mM respectively 288 mM was titrated into the sample. Which gave a final concentration of 36 mM respectively 72 mM DDM.

3.2 Methods

An optimization of the methods below was done in order to obtain the appropriate settings and conditions. The optimization aimed to refine a method and ensure accurate and reliable results.

3.2.1 AF4

Agilent Technologies is the manufacturer of the AF4 instrument used. For each run with the AF4 instrument a mini channel of 115 mm was used together with a membrane of regenerated cellulose with a molecular weight cut off at 10 kDa and a spacer of 480 µm. Before injecting any samples, the channel was conditioned for 5 hours with a detector flow and cross flow at 0.5 ml/min. The channel was then validated by inject bromophenol blue, which is a coloured sample. Finally, a focus test of the coloured sample was performed.

The method used with the AF4 instrument is stated in table 1 and took a total of 36 minutes. Additionally, the detector flow was at 1.5 ml/min and the cross flow at 0.7 ml/min which was constant. The injected sample volume was 100 µl for all samples which makes the total mass of injected trastuzumab equal for all runs. To the instrument a UV detector and a Multi-Angle Light Scattering detector was installed which measured each run and the software program Astra was used in order to save and analyse the data obtained.

Table 1: Time table settings for AF4 when using trastuzumab.

Mode	Duration [min]	Cross Flow Start [ml/min]	Cross Flow End [ml/min]
Elution	1	0.7	0.7
Focus	1	0.7	0.7
Focus Inject	5	0.7	0.7
Focus	2	0.7	0.7
Elution	17	0.7	0.7
Elution	5	0.0	0.0
Elution Inject	5	0.0	0.0

3.2.2 DLS

Wyatt is the manufacturer for the DLS instrument used. During the experiment a 96-well plate was used for placement of each sample. The temperature was set to 25 °C and the instruments default settings were used which took 20 measurements of each sample each run. Each run took approximately 2 minutes. Additionally, each sample in the wells were measured twice. To save and analyse the obtained data the software DYNAMICS was used.

3.2.3 Fluorescence spectroscopy & static light scattering

Both the fluorescence spectroscopy and the static light scattering was measured simultaneously with an instrument manufactured by Probe Drum. The fluorescence was measured at 280 nm, while the static light scattering used a laser at 637 nm. For each run 200 µl titrant was titrated into a sample of 600 µl with steps of 5 µl and an equilibrium time of 30 seconds. The sample was placed in a kyvett and a magnet loop was used to stir the sample as the titrant was added. The software PD viewer was used in order to collect and analyse the data obtained.

4 Results

The following section presents the key findings of the research conducted in this master thesis.

4.1 AF4

As seen in figure 1, 3 and 5, the peak area is lower when having SDS in the sample compared to when only trastuzumab is present in the sample. Which means that the concentration of trastuzumab is lower. However, the same mass of protein have been injected, indicating that some of the protein is lost. It is also a trend seen in figure 1, 3 and 5 that when increasing the DDM concentration the peak returns more to its original state and looks more like the sample containing only trastuzumab. Which means that the concentration of detected trastuzumab is rising.

It is also a trend seen in figure 3 and 5, that when increasing the SDS concentration and still have low DDM concentration the peak differs in regards of number of peaks or retention time from the higher concentrations with DDM and the original sample.

Normalisation of the curves are seen in figure 2, 4 and 6 and allows comparison of the different samples without influence of differences in concentration. Instead, the elution profile could be compared directly. In figure 2 with the lowest SDS concentration the elution is similar to native trastuzumab, but elutes about one minute faster. In figure 4 and 6 where the SDS concentration is higher, it becomes even more clear that the two lowest concentrations of DDM have a different elution curve compared to native trastuzumab. While the samples with the two highest concentration of DDM have an elution curve more like native trastuzumab. Generally, it can be seen that with increasing DDM concentration the elution curve returns more to its original shape in terms of longer retention time and shape of the curve.

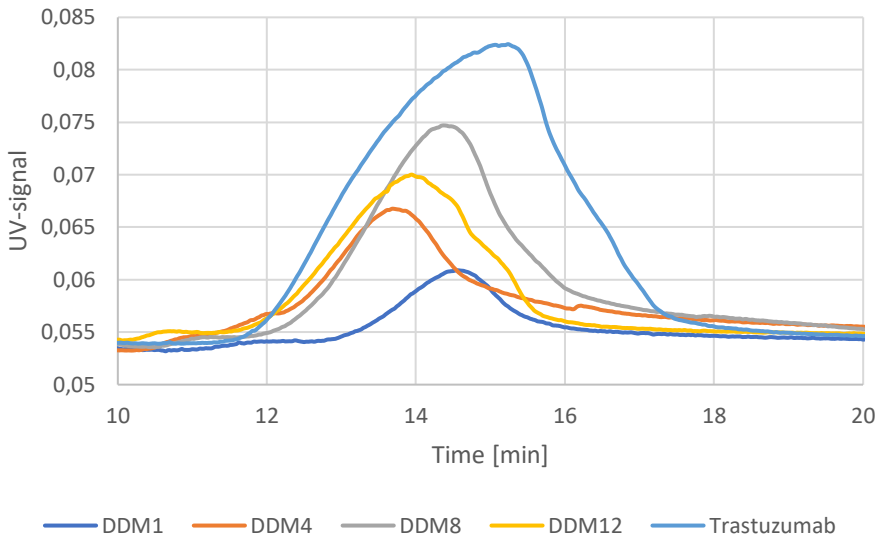

Figure 1: AF4 results of samples containing 3.8 mM SDS and 1 mg/ml trastuzumab with different DDM concentrations, 1:1, 1:4, 1:8 and 1:12. Except from the blue line which is a reference only containing trastuzumab in the sample.

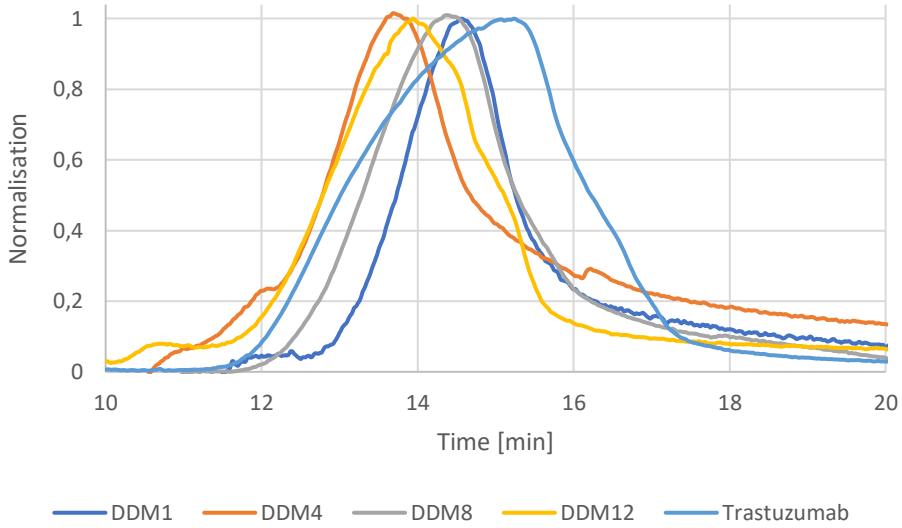

Figure 2: Normalisation of AF4 results of samples containing 3.8 mM SDS and 1 mg/ml trastuzumab with different DDM concentrations, 1:1, 1:4, 1:8 and 1:12. Except from the blue line which is a reference only containing trastuzumab in the sample.

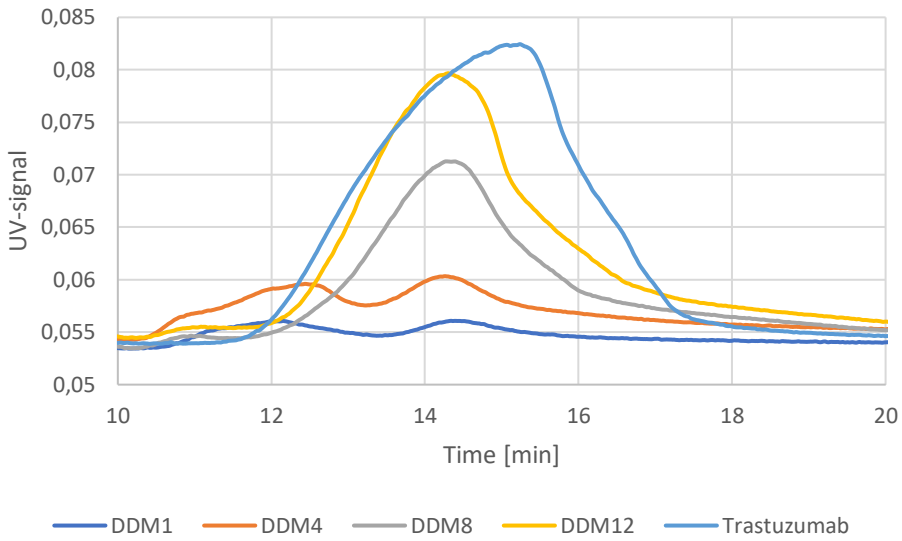

Figure 3: AF4 results of samples containing 6.25 mM SDS and 1 mg/ml trastuzumab with different DDM concentrations, 1:1, 1:4, 1:8 and 1:12. Except from the blue line which is a reference only containing trastuzumab in the sample.

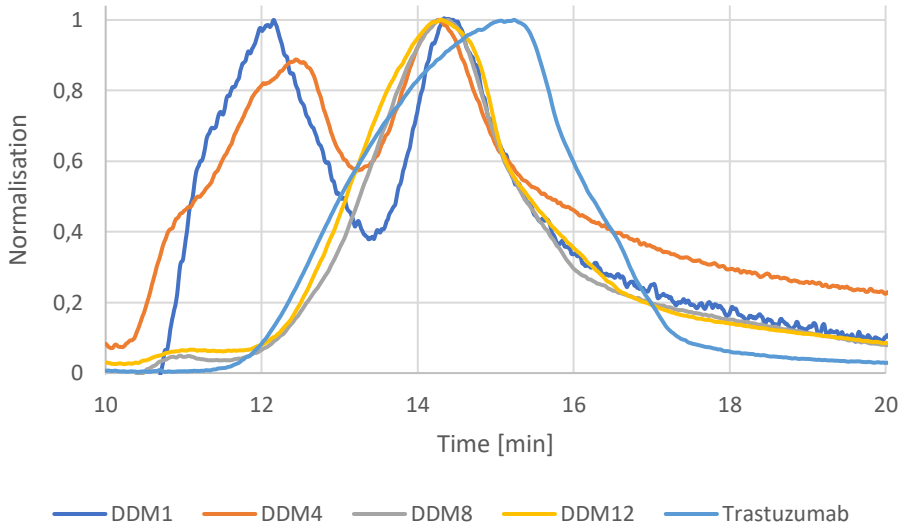

Figure 4: Normalisation of AF4 results of samples containing 6.25 mM SDS and 1 mg/ml trastuzumab with different DDM concentrations, 1:1, 1:4, 1:8 and 1:12. Except from the blue line which is a reference only containing trastuzumab in the sample.

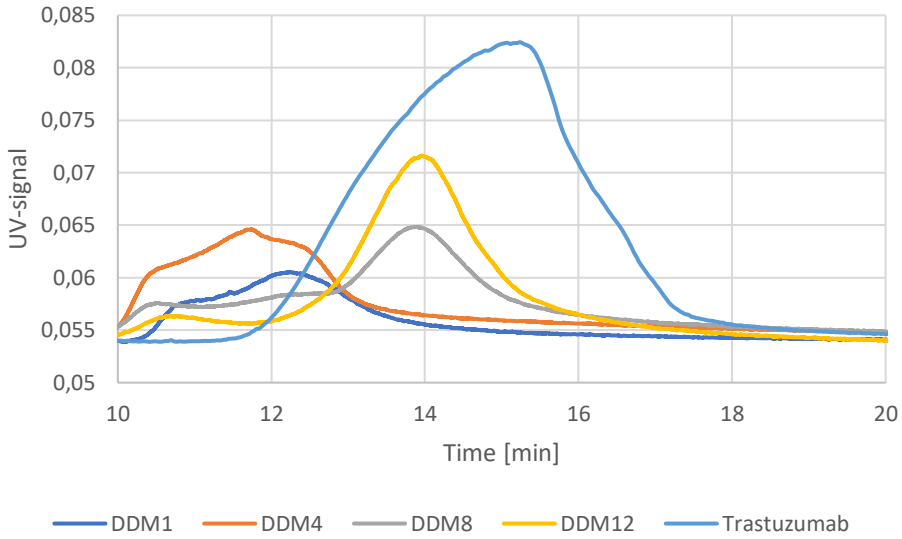

Figure 5: AF4 results of samples containing 12 mM SDS and 1 mg/ml trastuzumab with different DDM concentrations, 1:1, 1:4, 1:8 and 1:12. Except from the blue line which is a reference only containing trastuzumab in the sample.

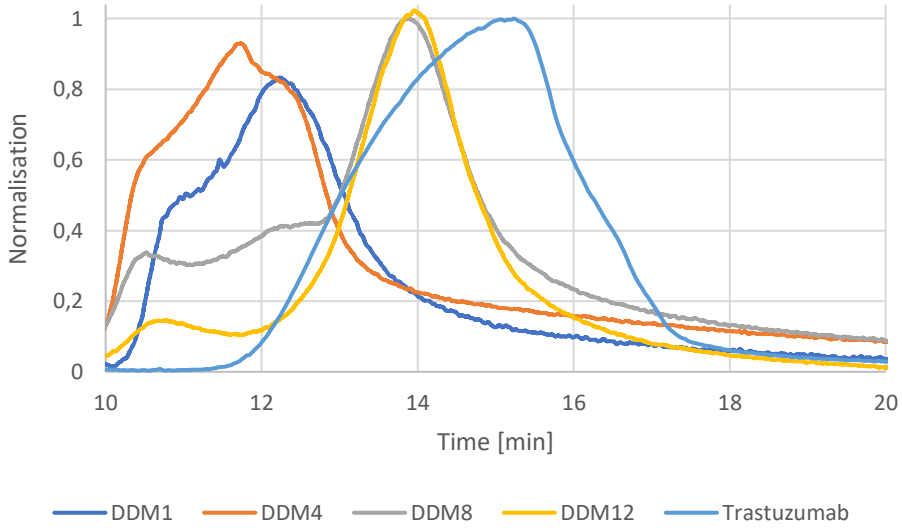

Figure 6: Normalisation of AF4 results of samples containing 3.8 mM SDS and 1 mg/ml trastuzumab with different DDM concentrations, 1:1, 1:4, 1:8 and 1:12. Except from the blue line which is a reference only containing trastuzumab in the sample.

4.2 DLS

As seen in figure 7, for the two highest concentrations of DDM with SDS:DDM ratio 1:8 and 1:12, two populations seem to emerge. It is seen that there is a constant radius population for all samples around 5 nm which is constant. The second population seems to be bigger for higher DDM concentrations than for lower.

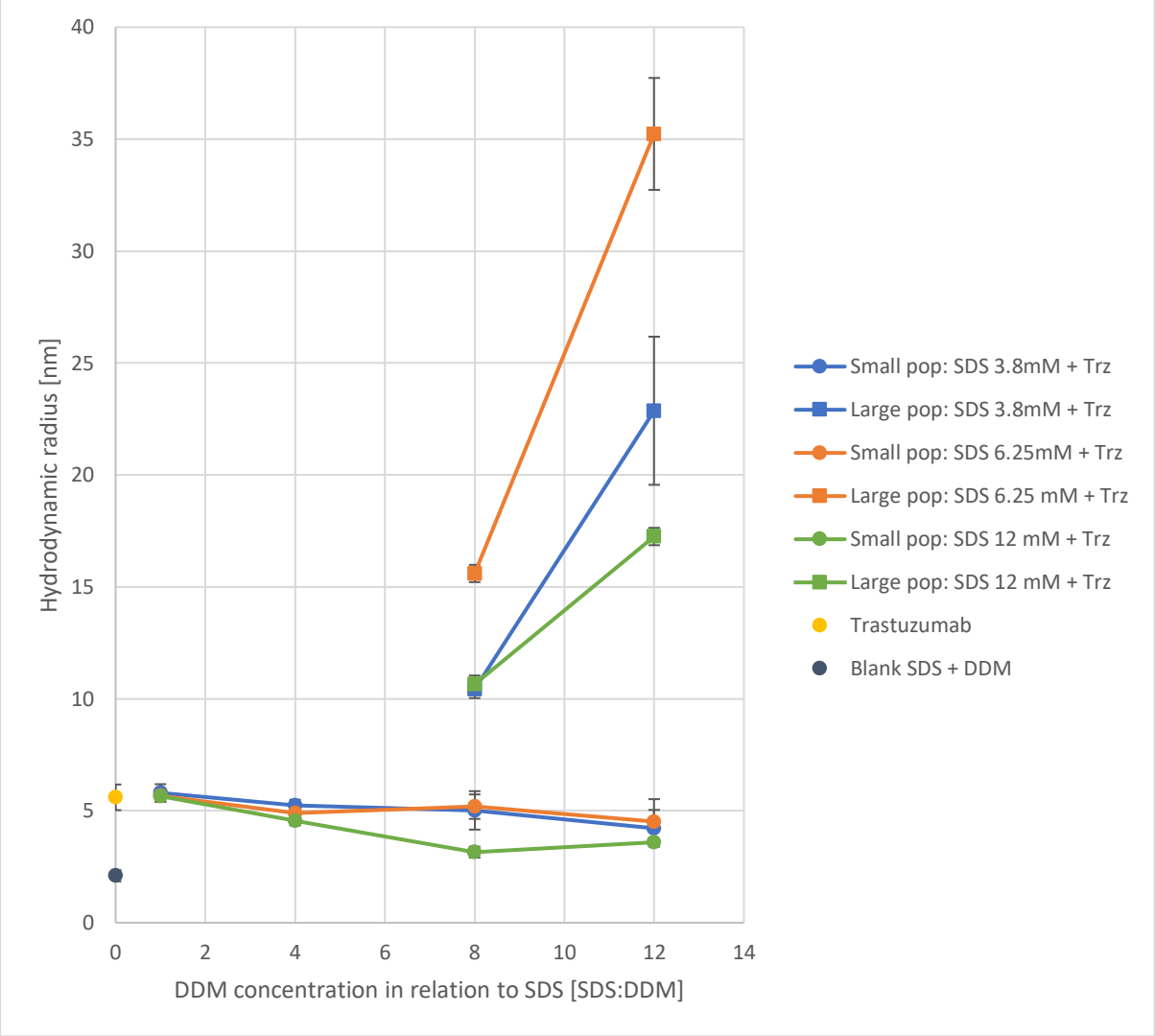

Figure 7: Hydrodynamic radius with standard deviation error bars of the different samples with different DDM concentrations marked as 1:1, 1:4, 1:8 and 1:12 on the x-axis. The large population and small population within the same sample are marked with squares and circles.

4.3 Fluorescence spectroscopy & static light scattering

As seen in figure 8, the fluorescence decreased rapidly when having only trastuzumab in the sample and SDS was added. When the molar ratio SDS:Trz reached 790:1 the fluorescence became rather constant. The figure also displays that when having trastuzumab and SDS in the sample, the fluorescence first increased and followed by a decrease as the DDM concentration raised in the sample. The maximal signal was reached when the molar ratio SDS:DDM was 1:5. It also shows that the fluorescence signal when adding DDM follows the same trend and reaches its maximum at the same molar ratio. However, the signal is increased with higher SDS and DDM concentration.

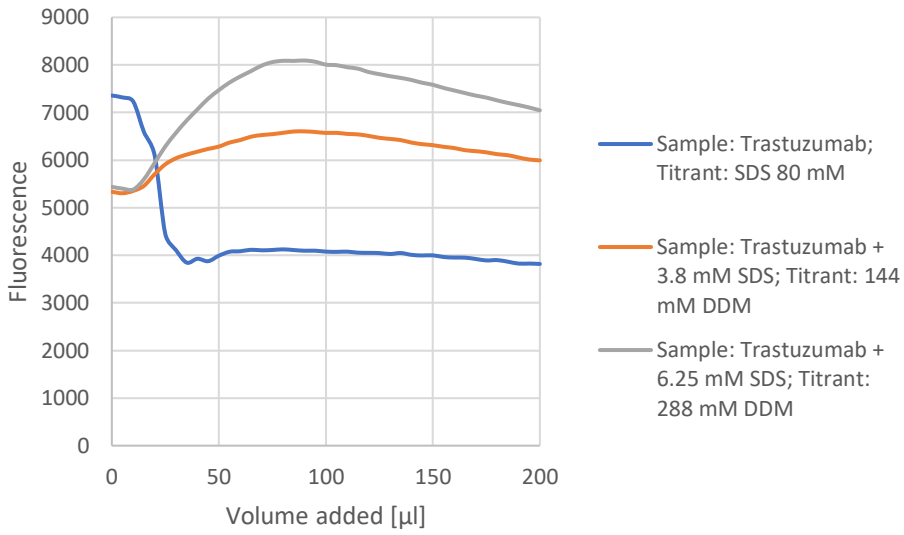

Figure 8: Fluorescence at 340 nm for trastuzumab dependent on SDS and DDM concentration.

As seen in figure 9, the scattering signal at 637 nm made a rapid increase when having only trastuzumab in the sample and SDS was added. The increase starts when the molar ratio SDS: DDM is 1.6:1 and when the molar ratio reaches 1:3.5 the signal has decreased and are slightly higher than it began at and remains rather constant. For both samples that were titrated with DDM, the signal is constantly increasing with time.

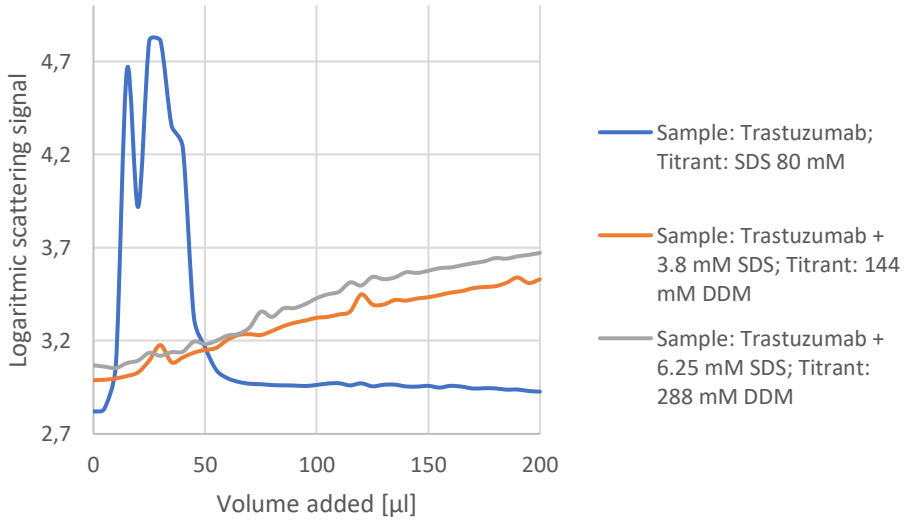

Figure 9: Logarithmic scattering signal at 637 nm for trastuzumab dependent on SDS and DDM concentration.

5 Discussion

From AF4 it is seen in figure 1, 3 and 5 that the signal is decreasing and the peak is not as wide when adding SDS compared to when only having pure trastuzumab in the sample, meaning the detected concentration is lower. This indicates that even if the mass trastuzumab injected from the sample is the same, not all the trastuzumab is eluting or it is precipitated in the sample vial. However, it is also seen that when increasing the amount of DDM in the sample, the curve is slowly returning to the appearance as when only trastuzumab is present, hence the concentration is increasing. This indicates that SDS will denaturate the protein in such a way that it either is not fully injected or becomes so large that it never reaches the detector before the time of each run is finished. Furthermore, it is seen from the shape of the elution curve seen in figure 2, 4 and 6 that DDM is reversing what SDS have done and more of the trastuzumab is in its native state as the DDM concentration is increased. The results indicates that DDM reverses the denaturation caused by SDS on trastuzumab in the same way as previous studies suggest (Otzen 2011, Kaspersen, et al. 2017, Otzen, et al. 2022). However, the protein is not fully returning to its native state which could be the result of several factors. Since the refolding occurs in several steps and takes longer time than unfolding (Pedersen, et al. 2020), not enough time for refolding could have been given. There might have not been DDM at high enough concentration to fully restore the protein to its native state, or there might have been traces of SDS tightly bound to the protein even after refolding (Buscajoni, et al. 2022).

For all curves containing SDS the elution is earlier compared to native trastuzumab, which is seen in figure 2, 4 and 6. When SDS denaturates the protein, its strucutre is lost, leading to a less ordered and more random-coil conformation. As a result, the protein could appear more compact than its native form. It is possible that the native form occupies more space due to its specific structure in order to be biological active. Therefore, the earlier elution could be because the denaturated protein is more compact than its native state.

For the two lower DDM concentrations in the run with SDS 6.25 mM and 12 mM seen in figure 4 and 6, the curve from AF4 do not follow the same elution pattern as the rest of the runs. When having 6.25 mM SDS in the sample, two peaks are appearing and when having 12 mM SDS in the sample, the peak are moved even further the left. This indicates that there is an issue with the measurement rather than that the size of trastuzumab have been decreased this much. The inaccurate results could be caused of a combination of low ionic strength in the carrier liquid as no salt was added together with high concentrations of SDS and not enough time for the sample to stabilise.

The DLS results from figure 7 shows that there is no significant change in the hydrodynamic radius when adding SDS and DDM to the sample and that it remains constant around 5 nm. However, at the higher concentrations of DDM and SDS, which are at or above their CMC two clear populations are formed. The smaller

population is at the radius 5 nm which indicates that it is trastuzumab in its native state. Some surfactants could be bound to the protein without it being seen on the DLS since they are so much smaller than the trastuzumab molecule. It can therefore not be concluded that no binding of surfactant is occurring even if the radius seems rather constant. The second population is larger and has a hydrodynamic radius between 10 nm and 35 nm. When increasing the surfactant concentration micelles will begin to form. How the micelle-protein surrounding looks cannot be established with DLS. However, it is likely because of the larger population size that several trastuzumab molecules are surrounding one micelle. It is also possible that one trastuzumab molecule will surround more than one micelle (Otzen, et al. 2022). The seconds populations size is of 2-7 trastuzumab molecules in their native state. However, the trastuzumab will unfold when denaturating, which could result in a longer molecule (Otzen, et al. 2022). This means that the larger population probably consists of even fewer trastuzumab molecules than 2-7. This indicates that as previous studies suggest, that the protein will interact with the micelles (Otzen 2011). However, more of the trastuzumab molecules should belong to the smaller population as the DDM concentration is increased (Kaspersen, et al. 2017), but this can not be seen with the DLS. The increasing size of the larger population as the DDM concentration is increasing does not necessarily suggest that there are more trastuzumab molecules interacting with the micelles. Even if this could be the case, it could also be as theory suggest that as more micelles forms and less protein are unfolded and interacting, each denaturated protein interacts with several micelles which increases its radius (Otzen 2011).

The results from fluorescence spectroscopy in figure 8 suggests that the fluorescence is decreasing when adding SDS to a sample of pure trastuzumab. While when adding DDM to a sample of trastuzumab containing SDS the fluorescence is instead increasing. This indicates that SDS will denaturate the protein which causes conformational changes that are seen by the decreasing signal, as the results from AF4 and theory suggests (Poghosyan, et al. 2019). However, the signal is increasing when adding DDM to the sample which indicates that the conformational changes trastuzumab have undergone due to SDS are reversing and the protein is returning to its native state as expected (Kaspersen, et al. 2017). The increasing signal is maximal when the relationship between SDS and DDM is around 1:5 and then the signal is slightly decreasing but slowly becomes more constant. At the maximum the signal is higher than for native trastuzumab which could be caused by one of the several steps in the refolding process, more or larger micelles could be formed which also could be the cause. Over time, or with sufficient concentration of DDM the signal is slightly decreasing and is finally higher than initially but lower than for native trastuzumab. Which indicates that trastuzumab are partly restored to its native state or that some of the trastuzumab molecules are restored to their native state. This align with theory that suggest that DDM micelles are formed and that SDS molecules are inserted into those micelles which further decreases the denaturation of the protein (Otzen, 2011). Since the protein is not fully restored to its native state, it could be caused by not enough DDM (Kaspersen, et al. 2017) or that there has not been enough time for the refolding to occur before the measurements were taken (Pedersen, et al. 2020).

Furthermore, it can be seen from the static light scattering signal in figure 9, that there are large changes initially when adding SDS to the trastuzumab sample. Since this signal is later decreasing, it is likely from aggregation rather than conformational changes. However, when the signal has decreased, it is still higher than initially which indicates that the aggregation has been reversed and some confirmational change have occurred as expected (Poghosyan, et al. 2019). It is also seen that the signal is increasing for both samples when titrating with DDM. The increase seems too large for indicating confirmational changes, and it could instead be caused by more micelles present in the sample as the concentration increases.

A potential problem throughout the experiment could be that not enough time was given for DDM to reverse the conformational changes of trastuzumab caused by SDS. As previous findings suggest, the interaction is complex and the mechanism behind it is not yet fully established (Pedersen, et al. 2020). This indicates that the kinetics plays an important role for the refolding of the protein. Even if the samples of AF4 and DLS were given time for DDM to reverse the changes caused by SDS, the time given might not have been enough since the refolding sometimes is instant and sometimes takes longer times (Otzen, et al. 2022). However, this is probably a bigger issue for the fluorescence spectroscopy and the static light scattering results, as DDM is added rather quickly. It is therefore possible that the signal would increase further or not decrease if it was given more time to stabilise and refold before taking each measurement.

6 Conclusion

The results from both AF4, DLS and ProbeDrum shows that the ionic surfactant SDS are causing changes to the antibody trastuzumab. It can also be concluded that addition of the non-ionic DDM is reversing the changes SDS causes so the protein will partly return to its native state. Furthermore, it shows that by increasing the molar ratio of the non-ionic surfactant compared to the ionic surfactant, the effect will increase and more of the protein will return to its native state. It is also shown that the conformational changes caused by SDS are instant, while reversing them with DDM requires more time.

7 Future outlook

To further investigate the mechanism behind the protein-surfactant interactions and especially how non-ionic surfactants can reverse the conformational changes caused by ionic surfactant more studies would have to be done. To improve this study, it would be suggested to try even higher concentrations of DDM and SDS, as well as increase the stabilisation time before measurements are made. The study could also be performed with other ionic surfactants and other non-ionic surfactants in order to establish that this is not a phenomenon only caused by the specific surfactants SDS and DDM. Even if there have been similar studies with other proteins than trastuzumab it would be preferable to try even more proteins to establish the mechanism behind the interactions. Furthermore, it would be of great interest to get a more detailed picture of the mechanism behind it by using other methods such as NMR and SAX. Which would allow researchers to see the conformational changes and bindings in greater detail than in the methods and instruments used in this study.

8 References

Abedi, M., Cohan, R.A., Mahboudi, F., et al. (2019). MALDI-MS: a Rapid and Reliable Method for Drug-to-Antibody Ratio Determination of Antibody-Drug Conjugates. *Iranian Biomedical Journal* Volume 23 (Issue 6): Page 395-403. DOI: https://doi.org/10.29252/ibj.23.6.395

Buscajoni, L., Marinetz, M.C., Berkemeyer, M., et al. (2022). Refolding in the modern biopharmaceutical industry. *Biotechnology Advances* Volume 61. DOI: https://doi.org/10.1016/j.biotechadv.2022.108050

Cancercentrum. (2023). *Trastuzumab sc vid Bröstcancer*. https://kunskapsbanken.cancercentrum.se/lakemedelsregimer/brostcancer/trastuzumab-sc/patientinfo/ (2024-05-02).

Das, B., Kumar, B., Begum, W., et al. (2022). Comprehensive Review on Applications of Surfactants in Vaccine Formulation, Therapeutic and Cosmetic Pharmacy and Prevention of Pulmonary Failure due to COVID-19. *Chemistry Africa* Volume 5 (Issue 3): Page 459-480. DOI: https://doi.org/10.1007/s42250-022-00345-0

Fatma, I., Sharma, V., Thakur, R.C., et al. (2021). Current trends in protein-surfactant interactions: A review. *Journal of Molecular Liquids* Volume 341. DOI: https://doi.org/10.1016/j.molliq.2021.117344

Kaspersen, J.D., Søndergaard, A., Madsen., D.J., et al. (2017). Refolding of SDS-Unfolded Proteins by Nonionic Surfactants. *Biophysical Journal* Volume 112 (Issue 8): Page 1609-1620. DOI: https://doi.org/10.1016/j.bpj.2017.03.013

Labbot. (2023). *Automate & Combine Proven Biophysical Techniques in a New Way*. https://www.labbot.bio/instrument#product-technologies (2024-05-01).

Malvern Panalytical. (2024). *Dynamic Light Scattering (DLS)*. https://www.malvernpanalytical.com/en/products/technology/light-scattering/dynamic-light-scattering (2024-05-01).

Maskos, M., Stauber, R.H. (2011). Characterization of Nanoparticles in Biological Environments. *Comprehensive Biomaterials* Volume 3: Page 329-339. DOI: https://doi.org/10.1016/B978-0-08-055294-1.00011-8

Otzen, D. (2011). Protein-surfactant interactions: A tale of many states. *Biochimica et Biophysica Acta (BBA) – Proteins and Proteomics* Volume 1814 (Issue 5): Page 562-591. DOI: https://doi.org/10.1016/j.bbapap.2011.03.003

Otzen, D.E. (2002). Protein Unfolding In Detergents: Effect of Micelle Structure, Ionic Strength, pH, and Temperature. *Biophysical Journal* Volume 83 (Issue 4): Page 2219-2230. DOI: https://doi.org/10.1016/S0006-3495(02)73982-9

Otzen, D.E., Pedersen, J.N., Rasmussen, H., et al. (2022). How do surfactants unfold and refold proteins?. *Advances in Colloid and Interface Science* Volume 308. DOI: https://doi.org/10.1016/j.cis.2022.102754

Pedersen, J.N., Lyngsø, J., Zinn, T., et al. (2020). A complete picture of protein unfolding and refolding in surfactants. *Chemical Science* Volume 11 (Issue 3): Page 699-712. DOI: https://doi.org/10.1039/C9SC04831F

Poghosyan, A.H., Scafer, N.P., Lyngsø, J., et al. (2019). Molecular dynamics study of ACBP denaturation in alkyl sulfates demonstrates possible pathway of unfolding through fused surfactant clusters. *Protein Engineering, Design and Selection* Volume 32 (Issue 4): Page 175-190. DOI: https://doi.org/10.1093/protein/gzz037

PubChem. *Dodecyl-beta-D-maltoside*. https://pubchem.ncbi.nlm.nih.gov/compound/Dodecyl-beta-D-maltoside (2024-05-01).

PubChem. *Sodium dodecyl sulfate*. https://pubchem.ncbi.nlm.nih.gov/compound/Sodium-dodecyl-sulfate (2024-05-01).

Sanches-Fernandes, A., Diehl, C., Houston, J., et al. (2020). An integrative toolbox to unlock the structure and dynamics of protein-surfactant complexes. *Nanoscale Advances* (Issue 9). DOI: https://doi.org/10.1039/D0NA00194E

ThermoFisher Scientific. (2024). *High-Purity Maltoside Detergents*. https://www.thermofisher.com/order/catalog/product/89902 (2024-05-02).

Umlong, I.M., Ismail, K. (2007). Micellization behaviour of sodium dodecyl sulfate in different electrolyte media. *Colloids and Surfaces A: Physicochemical and Engineering Aspects* Volume 299 (Issue 1-3): Page 8-14. DOI: https://doi.org/10.1016/j.colsurfa.2006.11.010

Xu, K., Lee, F., Gao, S., et al. (2015). Hylauronidase-incorporated hyaluronic acid-tyramine hydrogels for the sustained release of trastuzumab. *Journal of Controlled Release* Volume 2016: Page 47-55. DOI: https://doi.org/10.1016/j.jconrel.2015.08.015

9 Appendix

Below can background material be found to deepen the knowledge and understanding of the results and report be found.

Appendix A

The concentration of the trastuzumab sample given was determined with NanoDrop. The absorbances obtained from the experiment is listed in table 1. The concentration was given by applying the molar extinction coefficient, ε for trastuzumab which is 209409 M^{-1} cm^{-1} and its molar weight, M which is 145531,86 g/mol to the equation below (Abendi, et al. 2019). This gave an average value of 12.862 mg/ml.

$$A = \varepsilon \cdot M$$

Table 1: Absorbance of trastuzumab sample with unknown concentration obtained by NanoDrop.

Sample	Absorbance	Concentration [mg/ml]
1	17.586	12.222
2	17.744	12.331
3	18.117	12.591
4	17.653	12.268
5	19.324	13.429
6	18.978	13.189

References:
Abedi, M., Cohan, R.A., Mahboudi, F., et al. (2019). MALDI-MS: a Rapid and Reliable Method for Drug-to-Antibody Ratio Determination of Antibody-Drug Conjugates. *Iranian Biomedical Journal* Volume 23 (Issue 6): Page 395-403. DOI: https://doi.org/10.29252/ibj.23.6.395